Author(s): Narouz, Mina R.; Takano, Shinjiro; Lummis, Paul A.; Levchenko, Tetyana I.;
Nazemi, Ali; Kaappa, Sami; Malola, Sami; Yousefalizadeh, Goonay; Calhoun, Larry
A.; Stamplecoskie, Kevin G.; Häkkinen, Hannu; Tsukuda, Tatsuya; Crudden,
Cathleen M.

Title: Robust, Highly Luminescent Au13 Superatoms Protected by N-Heterocyclic Carbenes

Year: 2019

Version: Accepted version (Final draft)

JACS
JOURNAL OF THE AMERICAN CHEMICAL SOCIETY

Communication

Robust, Highly Luminescent Au13 Superatoms Protected by N-Heterocyclic Carbenes

Mina R. Narouz, Shinjiro Takano, Paul A. Lummis, Tetyana I. Levchenko, Ali Nazemi, Sami Kaappa, Sami Malola, Goonay Yousefalizadeh, Larry A. Calhoun, Kevin G. Stamplecoskie, Hannu Häkkinen, Tatsuya Tsukuda, and Cathleen M. Crudden

Just Accepted

Robust, Highly Luminescent Au₁₃ Superatoms Protected by N-Heterocyclic Carbenes

Mina R. Narouz,[†] Shinjiro Takano,[¶] Paul A. Lummis,[†] Tetyana I. Levchenko,[†] Ali Nazemi,[†] Sami Kaappa,[fl] Sami Malola,[fl] Goonay Yousefalizadeh,[†] Larry A. Calhoun,[£] Kevin G. Stamplecoskie,[†*] Hannu Häkkinen,[fl*] Tatsuya Tsukuda,[¶§*] and Cathleen M. Crudden[†‡*]

[†]Department of Chemistry, Queen's University, Chernoff Hall, Kingston, Ontario, Canada, K7L 3N6. [¶]Department of Chemistry, School of Science, The University of Tokyo, 7-3-1 Hongo, Bunkyo-ku, Tokyo 113-0033, Japan. [§]Elements Strategy Initiative for Catalysts and Batteries (ESICB), Kyoto University, Katsura, Kyoto 615-8520, Japan. [fl]Departments of Chemistry and Physics, Nanoscience Center, University of Jyväskylä, 40014 Jyväskylä, Finland. [‡]Institute of Transformative Bio-Molecules (WPI-ITbM), Nagoya University, Chikusa, Nagoya, Japan, 464-8602.

Supporting Information Placeholder

ABSTRACT: Gold superatom nanoclusters stabilized entirely by *N*-heterocyclic carbenes (NHCs) and halides are reported. The reduction of well-defined NHC–Au–Cl complexes produces clusters comprised of an icosahedral Au₁₃ core surrounded by a symmetrical arrangement of 9 NHCs and 3 chlorides. X-ray crystallography shows that the clusters are characterized by multiple CH–π and π–π interactions, which rigidify the ligand and likely contribute to the exceptionally high photoluminescent quantum yields observed, up to 16.0 %, which is significantly greater than the most luminescent ligand-protected Au₁₃ superatom cluster. Density functional theory analysis suggests that clusters are 8-electron superatoms with a wide HOMO-LUMO energy gap of 2 eV. Consistent with this, the clusters have high stability relative to all-phosphine clusters.

Ligand-stabilized gold clusters with atomically precise sizes are an important new class of nano-scale materials.[1-3] Their metallic cores can be viewed as "superatoms" because their electronic structures exhibit atom-like quantization.[4] Among others, icosahedral Au₁₃ cores with a closed electron configuration of $(1S)^2(1P)^6$ and nominal charge of 5+ are ubiquitous[5-11] (Fig. 1A). The fundamental and size-specific physicochemical properties of these $(Au_{13})^{5+}$ superatoms are highly interesting, including visible (600–700 nm) photoluminescence with quantum yields of $\sim 10^{-3}$,[12-15] much higher than bulk gold (10^{-10}).

However, problems remain for real-world application of these nanomaterials, with the most fundamental issue being stability against aggregation. Phosphines are only weakly bound to $(Au_{13})^{5+}$ and can be removed relatively easily, leading to aggregation. Thiols and alkynes have specific,

unalterable bonding modes that enable rapid exchange including metal atoms,[3] all of which leads to decreased cluster stability (Fig. 1A).

Recently, we demonstrated that a related superatom, $(Au_{11})^{3+}$ in $[Au_{11}(PPh_3)_8Cl_2]^+$ could be stabilized dramatically by introduction of a single *N*-heterocyclic carbene (NHC) ligand[16] (Fig. 1B). Single crystal X-ray diffraction (SCXRD) analysis showed that the NHC forms a directional Au–C bond as in the Au–PR₃ bonds. Theoretical calculations indicated that this enhanced stability originates not only from the strong Au–C bond but also interaction of the wingtips of the NHCs with the underlying Au clusters.[17] Although NHCs are promising ligands[18-21] in materials chemistry, and have been valuable in the stabilization of coordination clusters,[22,23] only mixed NHC/phosphine clusters could be prepared by the exchange method described in 1B. Recent computational studies suggest that NHCs will be valuable ligands to tune the photophysical properties of superatom clusters.[24] The only other examples of NHC-stabilized Au superatom clusters are two Au₃ clusters described in seminal reports by Sadighi and Bertrand.[25] Herein, we describe the
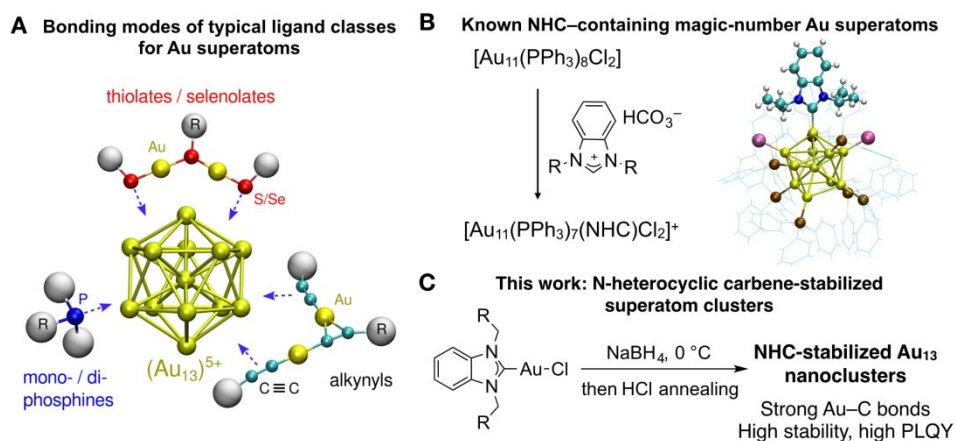

Fig. 1. Ligand stabilized Au₁₃ superatoms. (**A**) Known examples of icosahedral Au₁₃ superatoms stabilized by thiolate (RS), selenolate (RSe), alkynyl (RC≡C), mono- and di-phosphines (R₃P, R₅P₂). (**B**) Known example of Au₁₁ superatom structure stabilized by a single NHC. (**C**) One-pot, bottom up synthesis of NHC–stabilized Au₁₃ superatom by reduction of NHC–Au–Cl complexes.

first synthesis of NHC-protected Au_{13} superatoms by the direct reduction of NHC-Au(I)-Cl complexes. These clusters represent the first examples of Au superatom clusters larger than three atoms stabilized entirely by NHC and halide ligands.

The NHC-protected $(Au_{13})^{5+}$ superatoms showed much higher thermal stability than related phosphine complexes such as $[Au_{11}(PPh_3)_8Cl_2]^+$. SCXRD suggests that inter-ligand interactions in addition to a strong Au–C bond contribute to the stability. Interestingly, these NHC-protected superatoms exhibited visible photoluminescence at 730 nm with quantum yields (QY) up to 16.0 %, a remarkable number considering that the highest reported QY for Au_{13} superatom clusters of all types is 6.2%.[10] The high QY obtained herein is ascribed to a highly rigid structure, which suppresses non-radiative (vibrational) relaxation of excited states.[26-29]

Precursor NHC–Au–Cl complexes **2a-e** were produced easily and in high yield by the reaction of commercially available Me_2S–Au–Cl with benzimidazolium salts (**1a-e**) in the presence of K_2CO_3 (Fig. 2A).[30] Optimized conditions for cluster synthesis with **2a** employed $NaBH_4$ as the reducing agent at 0 °C, followed by warming to room temperature and treatment with HCl (Fig. 2B).[10] Examining the clusters by UV-vis absorbance spectroscopy and electrospray ionization mass spectrometry (ESI-MS) before and after HCl treatment showed that the crude material contained only molecular species and Au_{13} clusters, with no other significant cluster species detected. No significant changes were detected by ESI-MS after HCl treatment; the absorbance spectra, however, were significantly sharper (see Supporting Information).[31]

The molecular formula of cluster **3a** was determined to be $[Au_{13}(NHC^{Bn})_9Cl_3]^{2+}$, by ESI-MS analysis (Fig. 2C). This formula yields a gold core with eight delocalized electrons, in agreement with predictions from superatom theory,[4] and closely related to the cluster $[Au_{13}(NHC)_{10}Cl_2]^{3+}$ predicted by DFT.[17] Crystallization of cluster **3a** was achieved after anion exchange to yield the PF_6^- cluster $[3a][PF_6]_2$. As shown in Fig. 2D, the cluster is comprised of an icosahedral Au_{13} core with one gold atom at the center, with the remaining gold atoms bound to either chloride or NHC ligands.

NHC ligands are bound to the Au_{13} core via a single Au–C bond. The halide ligands take up a highly symmetrical arrangement, giving the cluster pseudo C_3 symmetry. The average Au–C bond length is 2.053(4) Å, consistent with previously reported NHC–Au complexes (see Supporting Information for full details). The average Au_{core}–Au_{Shell} bond distance of the icosahedral Au_{13} core in **3a** is 2.768 ± 0.024 Å, comparable to $[Au_{25}(SR)_{18}]^-$ (2.775 ± 0.009 Å),[5,6] $[Au_{25}(C\equiv CR)_{18}]^-$ (2.773 ± 0.021 Å),[8] $[Au_{19}(PR_3)_3(C\equiv CR)_9]^{2+}$ (2.787 ± 0.061 Å),[9] $[Au_{13}(P_2R_5)_5Cl_2]^{3+}$ (2.764 ± 0.034 Å),[10] and $[Au_{13}(PR_3)_{10}Cl_2]^+$ (2.769 ± 0.026 Å).[11] The cluster contains multiple CH–π and π–π interactions between the benzyl substituents and both rings of the benzannulated NHC core (Fig. 2E). The rigid arrangement of the ligands is likely responsible for the enhanced photophysical properties of these clusters (*vide infra*).

Through the use of ^{13}C labeled NHC precursors, we were able to identify the C–Au bonds as occurring in the 200–214 ppm range of the ^{13}C NMR spectrum. The number of signals observed in the cluster region is indicative of the presence of other regioisomers, that were not isolated by crystallography. This illustrates another advantage of the use of NHCs as ligands, namely that they provide a spectroscopic handle that is highly indicative of the precise structure, employing a bulk spectroscopic method. The precise structure of these regioisomers is currently under investigation.

Complexes **2b-2f** were subjected to the same reducing conditions. The procedure was found to be general, but sensitive to the steric constraints of the NHCs. For example, 2-naphthylCH_2– substituents were tolerated, with complex **2b** giving Au_{13} cluster $[Au_{13}(NHC^{Np})_9Cl_3]^{2+}$ (**3b**) in good yield. Au complexes **2c** and **2d** react cleanly, providing Au_{13} clusters $[Au_{13}(NHC^{pTol})_9Cl_3]^{2+}$ (**3c**) and $[Au_{13}(NHC^{mTol})_9Cl_3]^{2+}$ (**3d**). More hindered precursor **2e** gave polydisperse clusters **3e** containing monocationic Au_{13} clusters $[Au_{13}(NHC^{oTol})_8Cl_4]^+$, in which some of the NHCs have truncated wingtip groups, along with dimerized cluster $[Au_{25}(NHC^{oTol})_{10}Cl_7]^{2+}$ (see Supporting Information, Fig. S51). Complex **2f**, in which the benzyl substituent is replaced with a less flexible phenyl group, gives no nanoclusters.
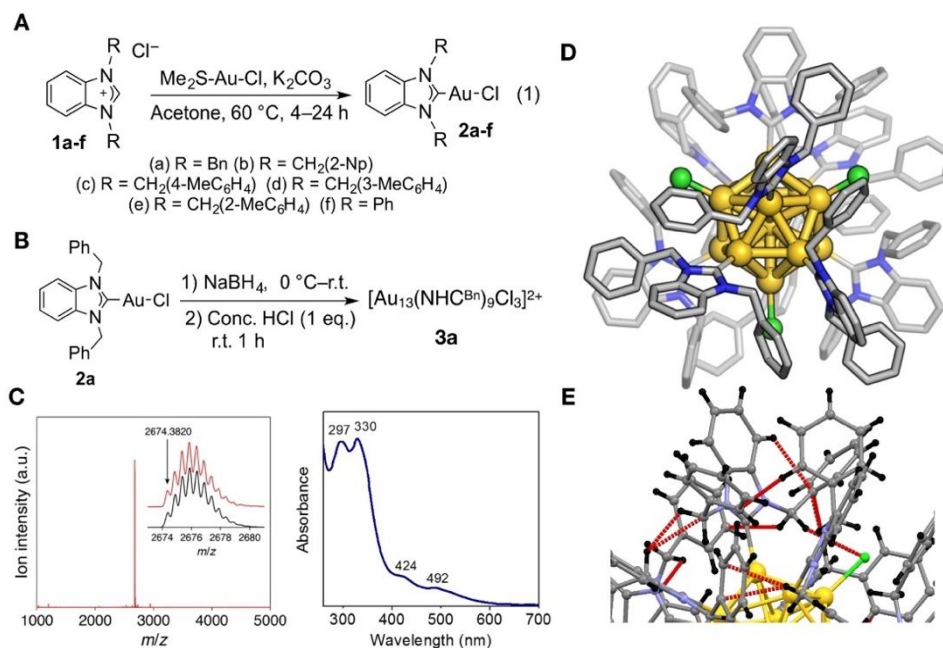

Fig. 2. Preparation and characterization of all-NHC Au_{13} nanoclusters. (**A**) Synthesis of NHC–Au–Cl complexes as monomeric precursors for nanoclusters. (**B**) Optimized conditions for the synthesis of $[Au_{13}(NHC)_9Cl_3]^{2+}$. (**C**) Characterization of nanoclusters by ESI–MS and UV-vis spectroscopy. (**D**) Single crystal X-ray crystallographically-determined structure of $[Au_{13}(NHC^{Bn})_9Cl_3]^{2+}$, (NHC = **1a**). Anions and hydrogen atoms have been removed, and wingtip phenyl rings shown as wireframe for clarity. Colour key: carbon (grey); nitrogen (blue); chlorine (green); gold (yellow). (**E**) Subset of inter-ligand CH–π interactions in **3a**, showing the high degree of organization of the ligand shell.

The thermal stability of these new clusters was assessed in hot acetonitrile. All-phosphine cluster $[Au_{11}(PPh_3)_8Cl_2]Cl$ (**4**)[32] was used as a benchmark, as it is one of the best characterized and most stable 8 electron superatom gold clusters stabilized by monodentate phosphines. As shown in Figs. 3A–C, **4** underwent full decomposition after 3 h, while NHC cluster **3a** showed only slight decomposition after 20 h, and cluster **3b** shows virtually no decomposition to nanoparticles, as judged by UV-vis absorbance spectroscopy. NMR analysis suggests that there may be some rearrangement of ligands on the surface, but ESI-MS analysis of

cluster **3a** after heating showed that the cluster was essentially unchanged, consistent with UV-vis absorbance studies. This improved stability is consistent with thermogravimetric analysis of the clusters, which demonstrates the loss of a single NHC at 180 °C and complete ligand loss at 585 °C. In contrast, ligand loss begins at 150 °C and is complete at 245 °C for cluster **4** (see Supporting Information).

The structural and electronic properties of **3a** and **3b** were examined by density functional theory (DFT), using the crystal structure of **3a** as a starting point (technical details in Supporting Information). The binding energy of the NHC ligand in **3a** was found to depend on the bonding site. A higher binding energy of about 2.3 eV was found to a gold site such as Au(2) in Fig. S54, which has chlorides bound to two neighboring Au sites. A lower binding energy of about 2.0 eV was found at Au(11) that has only one neighboring Au-Cl bond. These values were obtained by using the PBE functional; we found that the van der Waals corrections increased the binding energy by about 0.6 eV. For reference, PBE bonding energies of phosphine ligands to a related $[Au_{11}(PPh_3)_8Cl_2]^+$ cluster[16] were found to vary from 1.1 to 1.4 eV. This demonstrates that NHC binds to such gold clusters clearly stronger than phosphine.

When van der Waals interactions in the ligand layer were accounted for by using the BEEF-vdW functional, the predicted Au–NHC bond strength increased to 2.62 eV in **3a**. Compounds **3a** and **3b** have very similar HOMO–LUMO energy gaps of *ca.* 2.0 eV, reflecting the expected electronic stability of the 8-electron configuration (Figs. 3D–F, Supporting Information). Kohn-Sham orbitals near the Fermi level show distinct symmetry properties when projected to the Ih point group in the volume of the gold core (Figs. 3D and E). The HOMO, HOMO-1 and HOMO-2 states have triply degenerate T_{1u} symmetry corresponding to the p-type spherical orbitals as expected for an 8-electron superatom. The first few unoccupied states have e_g symmetry corresponding to five-fold degenerate d-states in spherical representation. Chlorine ligands break both the T_{1u} and e_g states by lowering the symmetry to C_3 (see Supporting Information).

The calculated UV-vis spectra of **3a** and **3b** were in good agreement with experimental data concerning the location of the optical gap and the visible absorption peaks (see Supporting Information). The superatom electronic structure predicts a dipole–allowed HOMO→LUMO transition as the lowest optical transition, which is confirmed in the spectral analysis. First excited states were examined by exciting an electron from the HOMO to the LUMO state by forcing the occupation numbers accordingly in the spin-polarized DFT calculation and relaxing the system with the PBE functional. The excited states of **3a** and **3b** were 1.68 eV and 1.61 eV higher in energy compare d to the ground state,
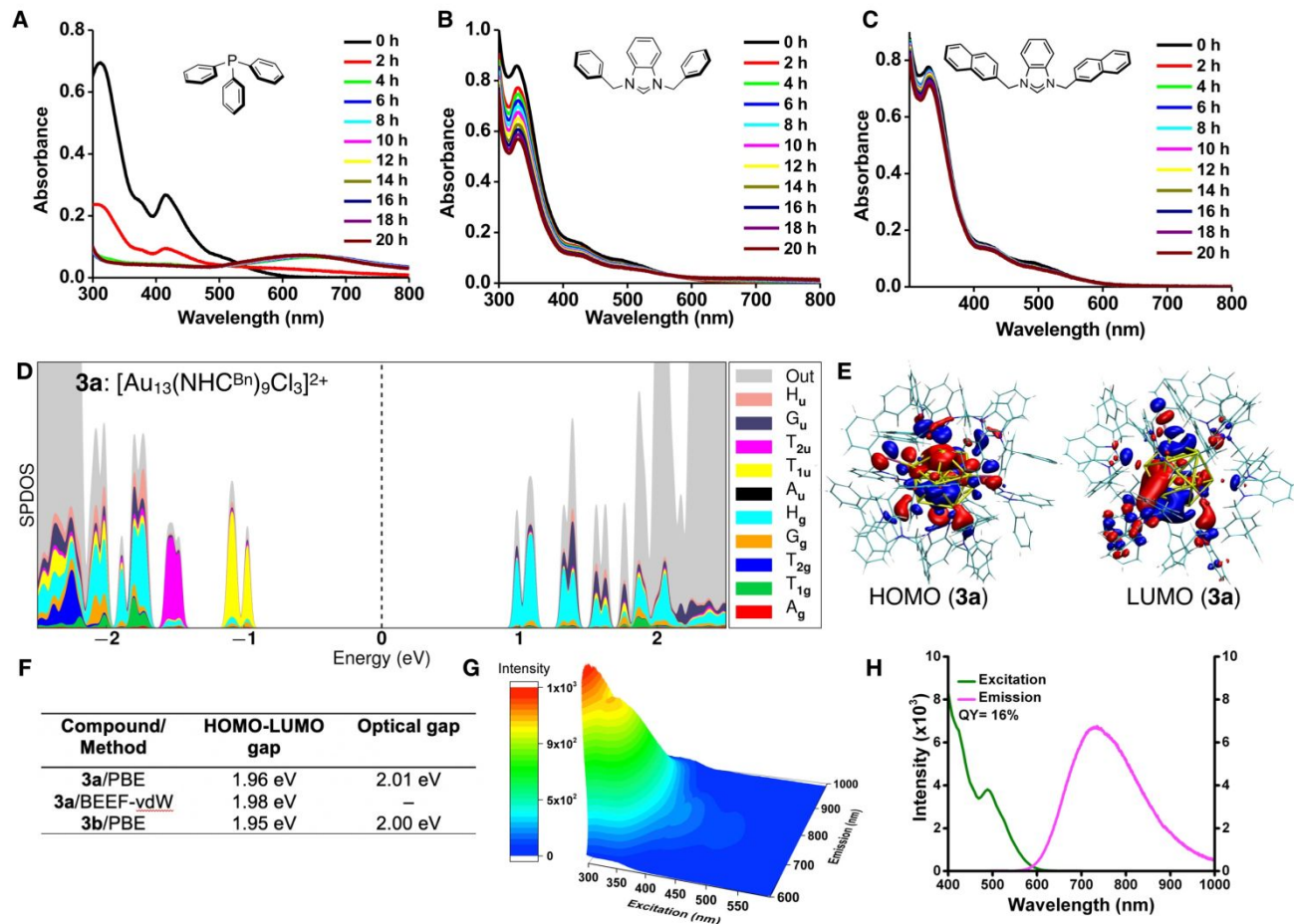

Fig. 3. Stability, optical properties and computational analysis of Au$_{13}$ clusters. A–C) UV-vis spectral study of Au clusters **4**, **3a** and **3b** before and after 20 h of heating in acetonitrile at 70 °C: (**A**) $[Au_{11}(PPh_3)_8Cl_2]Cl$ (**4**) from 0-20 h heating. (**B**) $[Au_{13}(NHC^{Bn})_9Cl_3]^{2+}$ (**3a**) from 0-20 h heating; (**C**) $[Au_{13}(NHC^{Np})_9Cl_3]^{2+}$ (**3b**) from 0-20 h heating. (**D**) I$_h$ symmetry-projected electronic density of states (SPDOS) of **3a**. Energy zero is at the center of the HOMO-LUMO gap. (**E**) Visualization of HOMO and LUMO orbitals for **3a**. (**F**) Comparison of DFT–predicted HOMO–LUMO gap with observed optical gap. (**G**) 3D fluorescence excitation–emission matrix spectra of **3b** illustrating the color and the high quantum yield of emission under visible and UVA light. (**H**) Fluorescence characterization of compound **3b**, Emission spectrum (with 485 nm excitation) and excitation spectrum (monitoring 730 nm emission) for **3b**.

respectively. These energies correspond to 738–770 nm in wavelength, in excellent agreement with observed emission spectra.

Fluorescence excitation–emission matrix (EEM) spectroscopy[33] studies of **3b** are shown in Figs. 3G and H. The excitation spectrum of **3b** matches very well with the absorbance spectrum for the same compound (Figs. 2E and 3H), indicating that the clusters are of high optical purity, and confirming that de-excitation of the superatom excited-state is responsible for the intense emission observed.[33] The quantum yield of fluorescence was determined from the EEM spectra (Fig. 3H) with excitation matched to the standard, zinc phthalocyanine. Clusters **3b** and **3a** boast impressive emission quantum yields of 16% and 7%, respectively, making these among the highest quantum yields ever recorded for Au_{13} superatoms.[10,12] More commonly, quantum yields for thiol-stabilized gold nanoclusters are <1%.[6,7,12] High emission quantum yields and blue shifted emission maxima, have been linked with electronic factors, although structural rigidity is also an important factor.[24] Femtosecond pump/probe spectroscopy (Fig. S67) confirms theoretical calculations that show the HOMO/LUMO transitions leading to the emissive excited state of **3b**. These preliminary results show a complete lack of dynamics for **3b**, consistent with a very rigid structure induced by the ligands, which have many internal π-stacking interactions. These interactions restrict the vibrational and rotational motion of ligands, limiting pathways for non-radiative decay processes. Cluster **3a** shows significant changes in the excited state following laser pulse excitation, as expected from a cluster with a lower emission quantum yield.

In conclusion, we have reported a simple, straightforward method to prepare NHC-stabilized superatom Au clusters. These clusters were shown to have higher stability than the corresponding phosphine clusters. Their HOMO-LUMO gaps, measured spectroscopically and computed with DFT, are approximately 2 eV, which is consistent with the high stability determined by thermal treatment and analysis by UV-vis absorbance and electrospray ionization mass spectrometry. In fluorescence studies, naphthyl–containing cluster **3b** was found to have a quantum yield of 16.0%, which is over twice that of the best reported Au_{13} superatom gold cluster.[10] This high quantum yield was attributed to a rigid NHC core, supported by a detailed analysis of molecular arrangement in benzyl derivative **3a**, and bodes well for future applications of these exciting, novel clusters.

ASSOCIATED CONTENT

Supporting Information

Experimental procedures and compound characterization, reaction monitoring by UV-vis spectroscopy and details of computational methodology. The Supporting Information is available free of charge on the ACS Publications website.

AUTHOR INFORMATION

Corresponding Authors

***Email**: Cathleen M. Crudden: cruddenc@chem.queensu.ca
Tatsuya Tsukuda: tsukuda@chem.s.u-tokyo.ac.jp
Hannu Häkkinen: hannu.hakkinen@jyu.fi
Kevin Stamplecoskie: kevin.stamplecoskie@queensu.ca

Notes

The authors declare no competing financial interests. Crystallographic data is available free of charge from the Cambridge Crystallographic Data Centre under reference number CCDC 1886732.

ACKNOWLEDGMENTS

REFERENCES

(1) Tsukuda, T.; Häkkinen, H. Protected Metal Clusters: From Fundamentals to Applications Elsevier: Amsterdam, 2015.

(2) Jin, R. C.; Zeng, C. J.; Zhou, M.; Chen, Y. X. Atomically Precise Colloidal Metal Nanoclusters and Nanoparticles: Fundamentals and Opportunities. *Chem. Rev.* **2016**, *116*, 10346–10413.

(3) (a) Chakraborty, I.; Pradeep, T. Atomically Precise Clusters of Noble Metals: Emerging Link Between Atoms and Nanoparticles. *Chem. Rev.* **2017**, *117*, 8208–8271; (b) Tang, Q.; Hu, G.; Fung, V.; Jiang, D.-E., Insights into Interfaces, Stability, Electronic Properties, and Catalytic Activities of Atomically Precise Metal Nanoclusters from First Principles. *Acc. Chem. Res.* **2018**, *51*, 2793-2802.

(4) Walter, M.; Akola, J.; Lopez-Acevedo, O.; Jadzinsky, P. D.; Calero, G.; Ackerson, C. J.; Whetten, R. L.; Grönbeck, H.; Häkkinen, H. A Unified View of Ligand-Protected Gold Clusters as Superatom Complexes. *Proc. Natl. Acad. Sci.* **2008**, *105*, 9157.

(5) Heaven, M. W.; Dass, A.; White, P. S.; Holt, K. M.; Murray, R. W. Crystal Structure of the Gold Nanoparticle $[N(C_8H_{17})_4][Au_{25}(SCH_2CH_2Ph)_{18}]$. *J. Am. Chem. Soc.* **2008**, *130*, 3754–3755.

(6) Zhu, M.; Aikens, C. M.; Hollander, F. J.; Schatz, G. C.; Jin, R. Correlating the Crystal Structure of A Thiol-Protected Au_{25} Cluster and Optical Properties. *J. Am. Chem. Soc.* **2008**, *130*, 5883–5885.

(7) Negishi, Y.; Kurashige, W.; Niihori, Y.; Nobusada, K. Toward the Creation of Stable, Functionalized Metal Clusters. *Phys. Chem. Chem. Phys.* **2013**, *15*, 18736–18751.

(8) Li, J.-J.; Guan, Z.-J.; Lei, Z.; Hu, F.; Wang, Q.-M. Same Magic Number but Different Arrangement: Alkynyl-Protected Au_{25} with D_3 Symmetry. *Angew. Chem., Int. Ed.* **2019**, *58*, 1083–1087.

(9) Wan, X.-K.; Tang, Q.; Yuan, S.-F.; Jiang, D.-E.; Wang, Q.-M. Au_{19} Nanocluster Featuring a V-Shaped Alkynyl–Gold Motif. *J. Am. Chem. Soc.* **2015**, *137*, 652–655.

(10) Shichibu, Y.; Konishi, K. HCl-Induced Nuclearity Convergence in Diphosphine-Protected Ultrasmall Gold Clusters: A Novel Synthetic Route to "Magic-Number" Au_{13} Clusters. *Small* **2010**, *6*, 1216–1220.

(11) Briant, C. E.; Theobald, B. R. C.; White, J. W.; Bell, L. K.; Mingos, D. M. P.; Welch, A. J., Synthesis and X-ray Structural Characterization of the Centred Icosahedral Gold Cluster Compound $[Au_{13}(PMe_2Ph)_{10}Cl_2](PF_6)_3$; the Realization of a Theoretical Prediction. *J. Chem. Soc., Chem. Commun.* **1981**, 201–202.

(12) (a) Link, S.; Beeby, A.; FitzGerald, S.; El-Sayed, M. A.; Schaaff, T. G.; Whetten, R. L. Visible to Infrared Luminescence from a 28-Atom Gold Cluster. *J. Phys. Chem. B* **2002**, *106*, 3410–3415; (b) Kurashige, W.; Yamaguchi, M.; Nobusada, K.; Negishi, Y., Ligand-Induced Stability of Gold Nanoclusters: Thiolate versus Selenolate. *J . Phys. Chem. Lett.* **2012**, *3*, 2649-2652.

(13) Negishi, Y.; Nobusada, K.; Tsukuda, T. Glutathione-Protected Gold Clusters Revisited: Bridging the Gap Between Gold(I)−Thiolate Complexes and Thiolate-Protected Gold Nanocrystals. *J. Am. Chem. Soc.* **2005**, *127*, 5261–5270.

(14) Weerawardene, K. L. D. M.; Aikens, C. M. Theoretical Insights into the Origin of Photoluminescence of $Au_{25}(SR)_{18}^-$ Nanoparticles. *J. Am. Chem. Soc.* **2016**, *138*, 11202–11210.

(15) Yau, S. H.; Varnavski, O.; Goodson, T. An Ultrafast Look at Au Nanoclusters. *Acc. Chem. Res.* **2013**, *46*, 1506-1516.

(16) Narouz, M.R. Osten, K. M.; Unsworth, P. J.; Man, R. W. Y.; Salorinne, K.; Takano, S.; Tomihara, R.; Kaappa, S.; Malola, S.; Dinh, C.-T.; Padmos, J. D.; Ayoo, K.; Garrett, P. J.; Nambo, M.; Horton, J. H.; Sargent, E. H.; Häkkinen, H.; Tsukuda, T.; Crudden, C. M. N-Heterocyclic Carbene-Functionalized Magic-Number Gold Nanoclusters. *Nat. Chem.* **2019**, *11*, 419–425.

(17) Tang, Q.; Jiang, D.-E. Comprehensive View of the Ligand–Gold Interface from First Principles. *Chem. Mater.* **2017**, *29*, 6908–6915.

(18) Zhukhovitskiy, A. V.; Mavros, M. G.; Voorhis, T. V.; Johnson, J. A. Addressable Carbene Anchors for Gold Surfaces. *J. Am. Chem. Soc.* **2013**, *135*, 7418–7421.

(19) Crudden, C. M.; Horton, J. H.; Narouz, M. R.; Li, Z.; Smith, C. A.; Munro, K.; Baddeley, C. J.; Larrea, C. R.; Drevniok, B.; Thanabalasingam, B.; McLean, A. B.; Zenkina, O. V.; Ebralidze, I. I.; She, Z.; Kraatz, H.-B.; Mosey, N. J.; Saunders, L. N.; Yagi, A. Simple Direct Formation of Self-Assembled N-Heterocyclic Carbene Monolayers on Gold and their Application in Biosensing. *Nat. Comm.* **2016**, *7*, 12654.

(20) Crudden, C. M. Horton, J. H.; Ebralidze, I. I.; Zenkina, O. V.; McLean, A. B.; Drevniok, B.; She, Z.; Kraatz, H.-B.; Mosey, N. J.; Seki, T.; Keske, E. C.; Leake, J. D.; Rousina-Webb, A.; Wu, G. Ultra Stable Self-Assembled Monolayers of N-Heterocyclic Carbenes on Gold. *Nat. Chem.* **2014,** *6*, 409–414.

(21) Wang, G. Rühling, A.; Amirjalayer, S.; Knor, M.; Ernst, J. B.; Richter, C.; Gao, H.-J.; Timmer, A.; Gao, H.-Y.; Doltsinis, N. L.; Glorius, F.; Fuchs, H. Ballbot-Type Motion of N-Heterocyclic Carbenes on Gold Surfaces. *Nat. Chem.* **2017**, *9*, 152–156.

(22) Ube, H.; Zhang, Q.; Shionoya, M. A Carbon-Centered Hexagold(I) Cluster Supported by N-Heterocyclic Carbene Ligands. *Organometallics* **2018**, *37*, 2007–2009.

(23) Polgar, A. M.; Weigend, F.; Zhang, A.; Stillman, M. J.; Corrigan, J. F. A N-Heterocyclic Carbene-Stabilized Coinage Metal-Chalcogenide Framework with Tunable Optical Properties. *J. Am. Chem. Soc.* **2017**, *139*, 14045–14048.

(24) Muñoz-Castro, A., Potential of N-heterocyclic carbene derivatives from Au$_{13}$(dppe)$_5$Cl$_2$ gold superatoms. Evaluation of electronic, optical and chiroptical properties from relativistic DFT. *Inorg. Chem. Front.* **2019**, advance article. DOI: 10.1039/c9qi00513g

(25) (a) Robilotto, T. J.; Bacsa, J.; Gray, T. G.; Sadighi, J. P. Synthesis of a Trigold Monocation: an Isolobal Analogue of [H$_3$]$^+$. *Angew. Chem., Int. Ed.* **2012**, *51*, 12077–12080; (b) Jin, L.; Weinberger, D. S.; Melaimi, M.; Moore, C. E.; Rheingold, A. L.; Bertrand, G. Trinuclear Gold Clusters Supported by Cyclic(alkyl)(amino)carbene Ligands: Mimics for Gold Heterogeneous Catalysts. *Angew. Chem., Int. Ed.* **2014**, *53*, 9059–9063.

(26) Zheng, J.; Petty, J. T.; Dickson, R. M. High Quantum Yield Blue Emission from Water-Soluble Au$_8$ Nanodots. *J. Am. Chem. Soc.* **2003**, *125*, 7780–7781.

(27) Zheng, J.; Nicovich, P. R.; Dickson, R. M. Highly Fluorescent Noble-Metal Quantum Dots. *Annu. Rev. Phys. Chem.* **2007**, *58*, 409–431.

(28) Pyo, K.; Thanthirige, V. D.; Kwak, K.; Pandurangan, P.; Ramakrishna, G.; Lee, D. Ultrabright Luminescence from Gold Nanoclusters: Rigidifying the Au(I)–Thiolate Shell. *J. Am. Chem. Soc.* **2015**, *137*, 8244–8250

(29) Bootharaju, M. S.; Kozlov, S. M.; Cao, Z.; Shkurenko, A.; El-Zohry, A. M.; Mohammed, O. F.; Eddaoudi, M.; Bakr, O. M.; Cavallo, L.; Basset, J.-M. Tailoring the Crystal Structure of Nanoclusters Unveiled High Photoluminescence via Ion Pairing. *Chem. Mater.* **2018**, *30*, 2719–2725.

(30) Collado, A.; Gómez-Suárez, A.; Martin, A. R.; Slawin, A. M. Z.; Nolan, S. P. Straightforward Synthesis of [Au(NHC)X] (NHC = N-Heterocyclic Carbene, X = Cl, Br, I) Complexes. *Chem. Commun.* **2013**, *49*, 5541–5543.

(31) Note we cannot rule out the influence of smaller or less stable clusters that do not survive ESI-MS analysis.

(32) McKenzie, L. C.; Zaikova, T. O.; Hutchison, J. E. Structurally Similar Triphenylphosphine-Stabilized Undecagolds, Au$_{11}$(PPh$_3$)$_7$Cl$_3$ and [Au$_{11}$(PPh$_3$)$_8$Cl$_2$]Cl, Exhibit Distinct Ligand Exchange Pathways with Glutathione. *J. Am. Chem. Soc.* **2014**, *136*, 13426–13435.

(33) Ramsay, H.; Simon, D.; Steele, E.; Hebert, A.; Oleschuk, R. D.; Stamplecoskie, K. G. The Power of Fluorescence Excitation–Emission Matrix (EEM) Spectroscopy in the Identification and Characterization of Complex Mixtures of Fluorescent Silver Clusters. *RSC Adv.* **2018**, *8*, 42080–42086.

SYNOPSIS TOC